Solar Phys (2009) 256: 167–181
DOI 10.1007/s11207-009-9344-7

Geometric Localization of CMEs in 3D Space Using STEREO Beacon Data: First Results

Curt A. de Koning · V.J. Pizzo · D.A. Biesecker

Received: 10 December 2008 / Accepted: 25 March 2009 / Published online: 17 April 2009

Abstract The geometric localization technique (Pizzo and Biesecker, *Geophys. Res. Lett.* **31**, 21802, 2004) can readily be used with *Solar Terrestrial Relations Observatory* (STEREO) Space Weather Beacon data to observe coronal mass ejection (CME) propagation within three-dimensional space in near-real time. This technique is based upon simple triangulation concepts and utilizes a series of lines of sight from two space-based observatories to determine gross characteristics of CMEs, such as location and velocity. Since this work is aimed at space weather applications, the emphasis is on use of COR2 coronagraph data, which has a field of view from $2.5R_{\odot}$ to $15R_{\odot}$; this spatial coverage allows us to observe the early temporal development of a CME, and hence to calculate its velocity, even for very fast CMEs. We apply this technique to highly-compressed COR2 beacon images for several CMEs at various spacecraft separation angles: 21 August 2007, when the separation angle between the two spacecraft was 26°; 31 December 2007 and 2 January 2008, when the separation angle was 44°; and 17 October 2008, when the spacecraft separation was 79°. We present results on the speed and direction of propagation for these events and discuss the error associated with this technique. We also compare our results to the two-dimensional plane-of-sky speeds calculated from STEREO and SOHO.

1. Introduction

A new 11-year cycle of heightened solar activity, bringing with it increased space weather risks, shows signs that it is on its way with the cycle's first sunspot, designated NOAA

STEREO Science Results at Solar Minimum
Guest Editors: Eric R. Christian, Michael L. Kaiser, Therese A. Kucera, O.C. St. Cyr.

C.A. de Koning (✉)
Cooperative Institute for Research in Environmental Sciences, University of Colorado, Boulder, CO, USA
e-mail: curt.a.dekoning@noaa.gov

C.A. de Koning · V.J. Pizzo · D.A. Biesecker
NOAA/Space Weather Prediction Center, Boulder, CO, USA

AR10981, appearing in the Sun's northern hemisphere on 4 January 2008. Furthermore, the likely passage of solar minimum during the summer of 2008 suggests the imminent onset of solar cycle 24. Manually cataloged coronal mass ejection (CME) data (Yashiro *et al.*, 2004) from solar cycle 23, observed by the Large Angle and Spectrometric Coronagraph (LASCO) (Brueckner *et al.*, 1995) experiment onboard the *Solar and Heliospheric Observatory* (SOHO) (Domingo, Fleck, and Poland, 1995), suggests that once the solar cycle begins we can expect a rapid increase in the number of partial and full halo CMEs. Such CMEs are typically considered important drivers of space weather as they can trigger geomagnetic storms (Gosling, 1990).

Space weather forecasters need to determine accurately whether a CME is Earth directed, and, if so, when the CME will impact Earth. To be useful, such a forecast must be made well before CME arrival at Earth. In other words, forecasters are not concerned with the structural details of CMEs; rather, they need to determine in near-real time the gross properties of Earth-directed CMEs, such as CME location, speed, and direction of propagation. Such a CME locater algorithm should be able to run in nearly automated mode within the National Oceanic and Atmospheric Administration (NOAA) Space Weather Prediction Center; therefore, the algorithm must be simple, robust, and easy to use. Recently, Pizzo and Biesecker (2004) have developed a straightforward geometric localization methodology, which can be used with STEREO white-light coronagraph observations, that meets these requirements. This technique is based upon simple triangulation concepts and utilizes a series of lines of sight from two space-based observatories to determine gross propagation characteristics of CMEs.

A variety of other methods are being explored to exploit STEREO image data, including, for example, inverse reconstruction using Pixon (Antunes, Thernisien, and Yahil, 2009), forward modeling (Thernisien, Howard, and Vourlidas, 2006), and polarization analysis (Moran and Davila, 2004). These methods are intended for CME research and rely on science-quality image data. In this paper, we use near-real time, highly-compressed, beacon data from STEREO to test the operational capability of the geometric localization technique for space weather forecasting of CMEs.

2. Data

The *Solar Terrestrial Relations Observatory* (STEREO) spacecraft (Kaiser *et al.*, 2008) were launched on 26 October 2006 at 00:52 UT. The science mission officially began on 21 January 2007 after completion of the phasing orbits that placed both spacecraft in heliocentric orbit. STEREO-A has a shorter orbital period than Earth and hence drifts ahead of Earth at an average rate of $\sim 22^\circ$ per year. Correspondingly, STEREO-B has a longer orbital period than Earth and thus lags Earth with a similar drift rate. Note that the drift rates vary throughout the mission (Driesman, Hynes, and Cancro, 2008).

White-light coronagraph data analyzed in this paper were observed by the Sun Earth Connection Coronal and Heliospheric Investigation (SECCHI) suite of instruments (Howard *et al.*, 2008). SECCHI comprises five telescopes, which together image the solar corona from the solar disk to beyond 1 AU. These telescopes are an extreme ultraviolet imager (EUVI: $1R_\odot - 1.7R_\odot$), two traditional Lyot coronagraphs (COR1: $1.5R_\odot - 4R_\odot$ and COR2: $2.5R_\odot - 15R_\odot$), and two so-called heliospheric imagers (HI-1: $15R_\odot - 84R_\odot$ and HI-2: $66R_\odot - 318R_\odot$). In this paper, we specifically use COR2 data to analyze CME propagation near the Sun. The large COR2 field of view, as compared to the COR1 field of view, allows us to observe the temporal development of a CME and hence calculate its velocity,

even for very fast CMEs. In addition, observations from COR2 beacon images have a sufficient signal-to-noise ratio so that we can reasonably identify the periphery of the CME from both spacecraft; such well-defined features may be absent in the HI beacon images.

The STEREO Space Weather Beacon mode is a continuous, real-time, low-data-rate (633 bits s^{-1}) broadcast of the data from STEREO. The allocation for the SECCHI space weather data is 500 bits s^{-1} (Biesecker, Webb, and St. Cyr, 2008). This very low data rate necessitates careful choices of the data to be telemetered, since the full STEREO data set cannot be downlinked in the beacon. Care has been taken to work with the instrument teams to ensure the resulting data will still be of value to the NOAA space weather forecasters. In particular, COR2 images are compressed using ICER, a lossy wavelet image compression scheme, and binned down from their original size of 2048×2048 pixels to 256×256 pixels. Although the beacon data are noisier than the science-quality data, the combined compression and binning schemes were designed to provide a sufficient signal-to-noise ratio for space weather forecasting. The COR2 beacon data are transmitted every 15 minutes. SECCHI images from the Space Weather Beacon undergo the exact same onboard processing, as well as processing at the STEREO Science Center (Eichstedt, Thompson, and St. Cyr, 2008), as the science-quality images.

2.1. Data Processing

The geometric localization tool consists of a single IDL program that can process any SECCHI image, whether science data or beacon data. Based on the time period of interest provided by the user, the program retrieves, processes, and displays a pair of concurrent coronagraph images taken by SECCHI-A and SECCHI-B. It is assumed that the images are stored on the user's computer in the `fits` (Flexible Image Transport System) file format. The user then manually selects the CME from each image, as shown in Figure 1. User intervention is necessary at this point because of the difficulty in automatically identifying the faint boundary of the CME as a whole, instead of the sharper edges associated with bright coronal features, such as, for example, streamer belts or structures internal to the CME.

Once the user has identified the region of interest from each of the two images, the geometric localization tool automatically applies several coordinate transformations. These transformations include corrections for projection effects applied to the raw pixel positions within the region of interest, using the IDL SolarSoft routine `wcs_get_coords`. This function returns a longitude and latitude in helioprojective coordinates, which is a spacecraft-centric system that gives the latitude and longitude of the original observations projected against the celestial sphere (Thompson, 2006). The helioprojective longitude and latitude can readily be transformed into a full three-dimensional Heliocentric Cartesian coordinate system, in which the xy-plane defines the spacecraft plane of sky and $\hat{z}$ points from the Sun to the spacecraft. A cyclic permutation of the axis labels transforms Heliocentric Cartesian coordinates into Heliocentric RTN coordinates. In RTN coordinates, $\hat{x}$ points away from Sun center through the spacecraft, $\hat{y}$ is formed by the cross product of the solar rotation axis and $\hat{x}$ and lies in the solar equatorial plane, and $\hat{z}$ is formed by the cross product of $\hat{x}$ and $\hat{y}$ and is the projection of the solar rotational axis on the plane of the sky. Finally, using the Stonyhurst heliographic longitude and latitude of the spacecraft, which is readily obtained from the metadata in the header that accompanies every `fits` image, we apply two coordinate system rotations and obtain the location of the observation in Heliocentric Earth Equatorial (HEEQ) coordinates. In this coordinate system, $\hat{z}$ is the solar rotation axis, $\hat{x}$ is in the plane containing the $\hat{z}$-axis and Earth, at the intersection of the solar central meridian and the heliographic equator, and $\hat{y}$ completes the right-handed coordinate system.

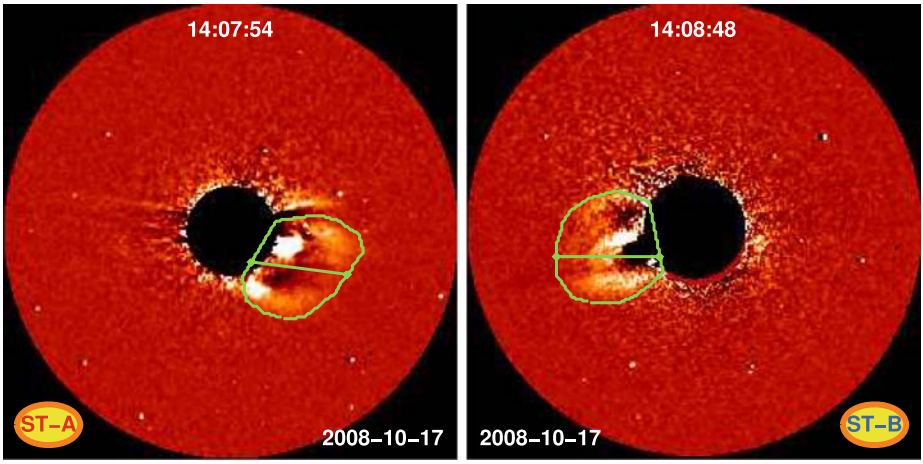

Figure 1 SECCHI/COR2 beacon data observed on 17 October 2008 at 14:08 UT. The green curve indicates the hand-drawn outline of the CME boundary used in the geometric localization calculation. The green line indicates one possible plane automatically chosen by the geometric localization program that contains both spacecraft.

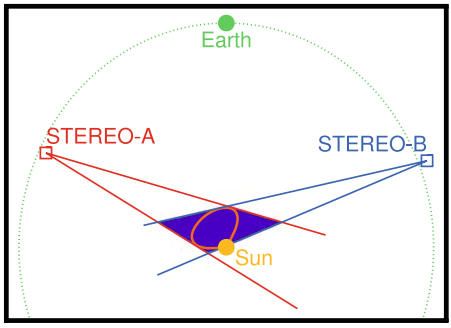

Figure 2 Schematic of the geometric localization technique applied within a common plane, that is, a plane containing both spacecraft that cuts through the two white-light images of the CME. The quadrilateral containing the CME is shown in purple.

With the spacecraft locations and the plane-of-sky information from both spacecraft in the same coordinate system, the program automatically chooses a plane that contains the spacecraft and cuts through the two white-light images of the CME, as shown in Figure 1 for a CME observed on 17 October 2008. Within the confines of this plane, the program draws a line from STEREO-A to the perceived edges of the CME as observed by STEREO-A. Similarly, the program draws a line from STEREO-B to the perceived edges of the CME as observed by STEREO-B. The intersection of the lines defines a quadrilateral that contains the CME, as shown in Figure 2. Repeated application of this process to various planes that slice through different sections of the two white-light CME images yields a stack of quadrilaterals that delimit the region occupied by the CME in three-dimensional space. Finally, by applying this technique to successive images, we can track the trajectory of the CME.

The geometric localization technique also works with a specific part of a CME, such as the leading-edge shell, provided that the substructures have distinct boundaries that appear in both images. Figure 3 shows the boundary, outlined in blue, for such a leading-edge shell for the CME observed on 17 October 2008.

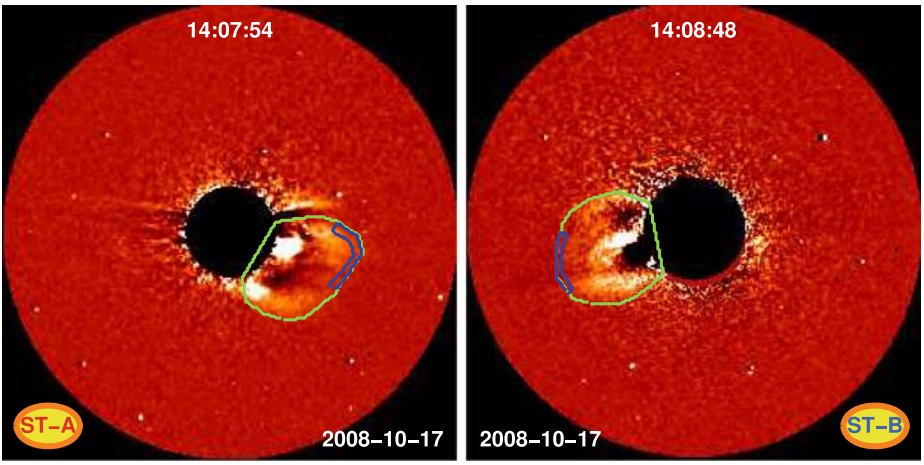

Figure 3 The same SECCHI/COR2 beacon data as shown in Figure 1. Once again, the green curve indicates the hand-drawn outline of the CME boundary used in the geometric localization calculation. The region inside the blue curve indicates the leading-edge shell.

Table 1 Positions of STEREO and Earth at 10:27 UT on 17 October 2008.

	STEREO-A	Earth	STEREO-B
Heliocentric radius (AU)	0.9643	0.9964	1.0740
Heliographic (HEEQ) longitude	40.512	0.000	−38.689
Heliographic (HEEQ) latitude	1.292	5.666	7.300
Separation angle with Earth	40.660		38.465
Separation angle A with B		79.125	

3. Description of Events

We apply the geometric localization technique to four CMEs at various spacecraft separation angles: 21 August 2007, when the separation angle between the two spacecraft was 26°; 31 December 2007 and 2 January 2008, when the separation angle was 44°; and 17 October 2008, when the spacecraft separation was 79°. We describe the 17 October 2008 event in significant detail to clearly explain the technique; the remaining events will be summarized briefly.

3.1. 17 October 2008

On 17 October 2008, both STEREO spacecraft and SOHO observed a CME. The CME onset in COR2-A occurred at 09:53 UT; in COR2-B the onset occurred at 10:24 UT. As shown in Figures 1 and 3, the CME appeared as a west-limb event in STEREO-A but as an east-limb event in STEREO-B. In addition, LASCO observed this event as a halo CME. The absence of space weather disturbances associated with this CME suggests that it was a backside halo event.

The positions of the STEREO spacecraft and Earth are listed in Table 1 and shown in Figure 4. The plots show the trajectories of Earth in green, STEREO-A in red, and STEREO-B in blue for a 20-day span centered on the day of the CME. The trajectories are plotted in

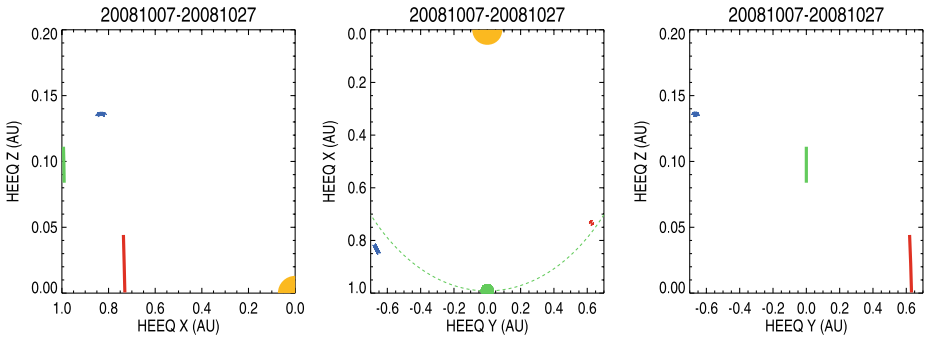

Figure 4 Location of STEREO spacecraft and Earth for a 20-day span centered on 17 October 2008; the trajectories of Earth and STEREO-A and STEREO-B are in green, red, and blue, respectively. In addition, the Sun is shown as a yellow circle.

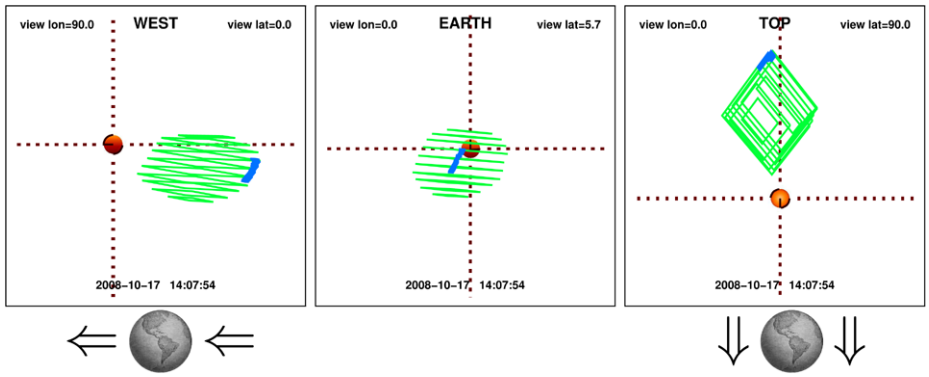

Figure 5 The three-dimensional spatial location of the CME on 17 October 2008 at 14:08 UT as calculated using geometric localization. The green quadrilaterals indicate the bounding volume of the CME as a whole; the blue quadrilaterals indicate the bounding volume of the leading-edge shell. The hash marks on the plots indicate the scale used; the distance between each mark is $1\,R_{\odot}$. The viewing latitudes and longitudes on the plots refer to the observer's position in HEEQ coordinates. The left plot is for an observer hovering over the west limb of the Sun; Earth is on the left-hand side of the plot. The center plot is for an observer at Earth. The right plot is for an observer looking down onto the north pole of the Sun; Earth is toward the bottom of the plot.

the HEEQ coordinate system and are shown in the xz-plane (left), xy-plane (center), and yz-plane (right). On this day, the two spacecraft were separated by $\sim$79°. This is close to the ideal spacecraft separation: When the spacecraft are separated by 80° – 100°, the quadrilateral area should be within 10% of the actual CME area (Pizzo and Biesecker, 2004).

Applying the geometric localization technique to observations of this event taken at 14:08 UT, shown in Figures 1 and 3, yields the three-dimensional spatial location shown in Figure 5. The quadrilaterals of the CME as a whole are shown in green; superimposed on this stack are blue quadrilaterals showing the location of the leading-edge shell outlined in Figure 3. To give a sense of the three-dimensional location, we show three views: The left plot is for an observer hovering over the west limb of the Sun; the center plot is for an observer at Earth; and the right plot is for an observer looking down onto the north pole of the Sun. The center plot clearly shows that the CME appeared as a halo event for an Earth-

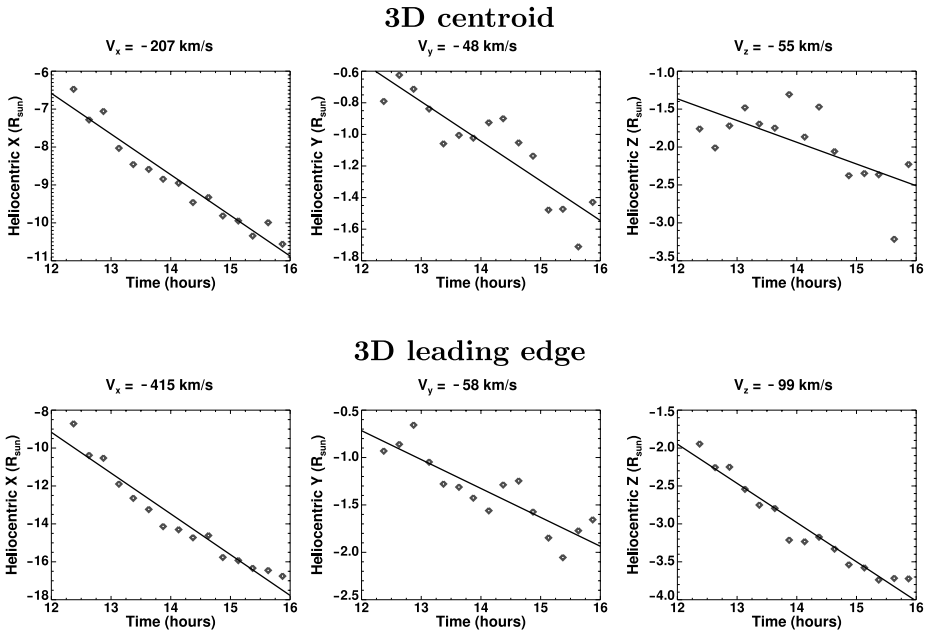

Figure 6 The three-dimensional velocity, in HEEQ coordinates, of the centroid (top row of plots) and leading edge (bottom row of plots) for the CME observed on 17 October 2008.

based observer, in agreement with LASCO observations. The results also confirm that this was indeed a backside halo event, in agreement with the lack of observed space weather activity.

The CME location calculated by geometric localization depends on a hand-drawn boundary. Another user, or even the same user at a later time, will draw a slightly different boundary, resulting in some variation in the CME location. This random error can be estimated by repeating the entire geometric localization technique multiple times for the same sequence of observations. When we do this we find an error of up to $0.3R_{\odot}$ in the centroid of the bounding volume for either the CME as a whole or the leading-edge shell.

Using geometric localization, we can obtain the speed and direction of propagation for this event. Figure 6 shows the position as a function of time for the centroid of the bounding volume of the CME (top row of plots) and the leading-edge shell (bottom row of plots). Although there is a large amount of scatter in the heliocentric-y position (the east – west direction), both sets of plots clearly indicate the CME was a backside event with a slight southerly trajectory. In particular, we find that the centroid speed was 232 ± 31 km s^{-1} with a propagation direction of $25 \pm 11°$S and $172 \pm 4°$E. Variations in the centroid location, owing to variations in the hand-drawn boundary, are reflected in the stated velocity errors. Once again, these random errors are estimated by repeating the entire geometric localization technique multiple times for the same sequence of observations. The leading-edge speed was 428 ± 44 km s^{-1} with a propagation direction of $13 \pm 2°$S and $178 \pm 4°$E.

Since SOHO observed this CME as a halo CME, the plane-of-sky speed measured from LASCO refers to the radial expansion of the CME, as opposed to the leading-edge speed, where $V_{\rm le} = V_{\rm cent} + V_{\rm rad}$. The LASCO CME catalog at the Catholic University of America (Yashiro *et al.*, 2004) reported a halo CME with a linear speed of 143 km s^{-1} for this date. In addition, the height – time plot in the catalog suggests that this CME underwent signif-

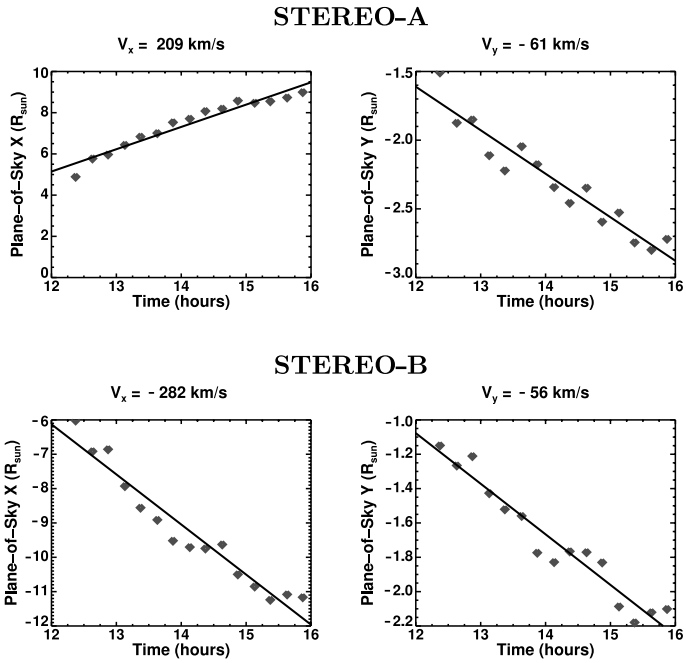

Figure 7 The plane-of-sky velocity of the leading edge for the CME observed by STEREO-A (top plots) and STEREO-B (bottom plots) on 17 October 2008.

icant acceleration out to at least $10R_{\odot}$. Although the plots of heliocentric-X versus time in Figure 6 suggests a nonlinear variation in the CME speed, we have not calculated an acceleration because, we believe, that the significant scatter in the Y and Z directions do not warrant a higher order fit. The Solar Eruptive Event Detection System (SEEDS) catalog (Olmedo *et al.*, 2008) used an 18°-wide portion of the halo in the 17 October 2008 event to calculate a radial expansion speed of 213 km s^{-1}. Using geometric localization, we calculate a radial expansion speed of 196 km s^{-1}, which falls in between the two catalog speeds.

For comparison, we also show the leading-edge plane-of-sky speed calculated for STEREO-A and STEREO-B in Figure 7. The plane-of-sky speed calculated from STEREO-A was 250 ± 23 km s^{-1}, whereas the plane-of-sky speed observed by STEREO-B was 255 ± 38 km s^{-1}. The calculated plane-of-sky speeds for this event obtained from the CACTus catalog (Robbrecht and Berghmans, 2004) were 231 km s^{-1} from STEREO-A and 312 km s^{-1} from STEREO-B. Our projected, two-dimensional plane-of-sky speeds are less than the fully three-dimensional speed, as expected. As a consistency check, we can derive the true spatial speed using $V_{\text{plane-of-sky}} = V_{3\text{D}} \cos\psi$, where ψ denotes the angle between the CME position obtained from geometric localization and the coronagraph plane of sky. STEREO-A returns a "true" speed of 400 km s^{-1} and STEREO-B returns 393 km s^{-1}, in good agreement with the geometric localization leading-edge speed, given the error estimate.

3.2. 2 January 2008

On 2 January 2008, both STEREO spacecraft observed an east-limb event. The CME onset in COR2-A occurred at 10:23 UT, whereas in COR2-B the onset occurred at 11:23 UT. This

Table 2 Positions of STEREO and Earth at 11:27 UT on 2 January 2008.

	STEREO-A	Earth	STEREO-B
Heliocentric radius (AU)	0.9674	0.9833	1.0113
Heliographic (HEEQ) longitude	21.139	0.000	−22.696
Heliographic (HEEQ) latitude	−5.401	−3.123	−0.051
Separation angle with Earth	21.202		22.891
Separation angle A with B		44.092	

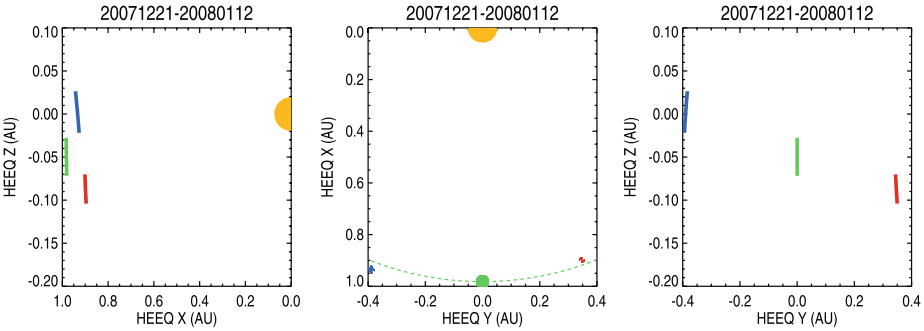

Figure 8 Location of STEREO spacecraft and Earth from 21 December 2007 to 12 January 2008. The use of colors is the same as in Figure 4.

CME, along with the other events discussed in the following, are morphologically similar to the 17 October 2008 CME; hence, we do not show further white-light coronagraph observations. At the time of the CME, the STEREO spacecraft and Earth were at the positions indicated in Table 2 and shown in Figure 8.

Applying the geometric localization technique to observations of this event taken at 12:38 UT yields the three-dimensional spatial location shown in Figure 9. These plots are similar to those shown in Figure 5, except that the right-hand plot is for an observer hovering over the east limb of the Sun, instead of the west limb. Notice also that Earth is to the right of the plot, instead of the left as in Figure 5.

Figure 10 shows the position as a function of time for the leading edge of the CME. The calculated speed was 640 ± 64 km s^{-1} and the propagation direction was $4 \pm 1°$S and $64 \pm 11°$E. Although not shown, the centroid speed for this event was 324 ± 45 km s^{-1} with a propagation direction of $1 \pm 10°$S and $67 \pm 14°$E. Therefore, the radial expansion for this CME was 316 km s^{-1}.

The leading-edge plane-of-sky speed calculated from STEREO-A was 648 ± 48 km s^{-1}, whereas the speed from STEREO-B was 412 ± 53 km s^{-1}. Correcting for projection effects returns a true spatial speed of 650 km s^{-1} from STEREO-A and 626 km s^{-1} for STEREO-B. These speeds agree quite well with the speed calculated by geometric localization. For comparison, CACTus identified a CME in COR2-A with a median speed of 520 km s^{-1} and a CME in COR2-B with a median speed of 416 km s^{-1}. In addition, SEEDS identified a CME in LASCO with a linear-fit speed of 350 km s^{-1} and the LASCO catalog lists a CME observed in C2 and C3 as a partial halo with a linear speed of 676 km s^{-1}.

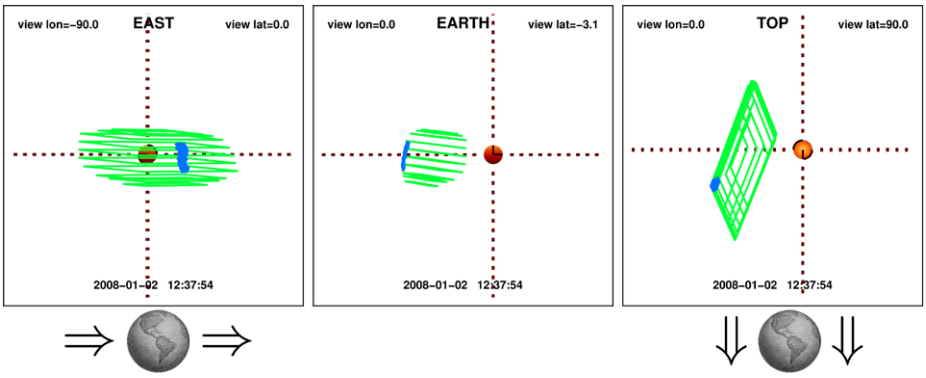

Figure 9 The three-dimensional spatial location of the CME on 2 January 2008 at 12:38 UT as calculated using geometric localization. These plots are similar to those shown in Figure 5, except that the left plot is for an observer hovering over the east limb of the Sun, instead of the west limb.

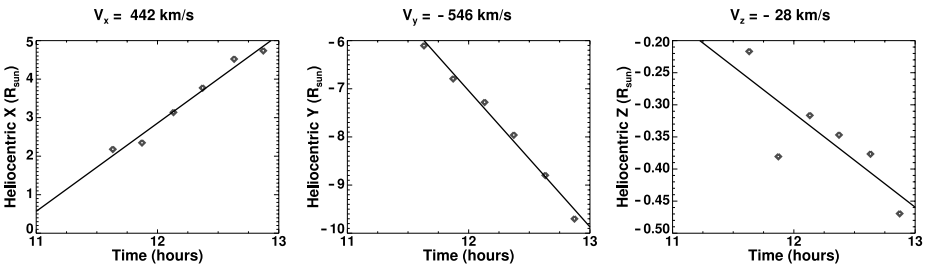

Figure 10 The three-dimensional velocity, in HEEQ coordinates, of the leading edge for the CME observed on 2 January 2008.

Table 3 Positions of STEREO and Earth at 01:23 UT on 31 December 2007.

	STEREO-A	Earth	STEREO-B
Heliocentric radius (AU)	0.9673	0.9833	1.0125
Heliographic (HEEQ) longitude	21.093	0.000	−22.599
Heliographic (HEEQ) latitude	−5.179	−2.839	0.251
Separation angle with Earth	21.169		22.801
Separation angle A with B		43.969	

3.3. 31 December 2007

Two days earlier, on 31 December 2007, the STEREO spacecraft also observed an east-limb event. The CME onset in both COR2-A and COR2-B occurred at 01:38 UT. At the time of the CME, the STEREO spacecraft and Earth were at the positions indicated in Table 3 and shown in Figure 8.

This CME was nearly in the plane of sky, as seen from Earth. The leading-edge speed for this event was 724 ± 51 km s^{-1} and the propagation direction was $3 \pm 2°$N and $96 \pm 6°$E, whereas the centroid speed was 491 ± 36 km s^{-1} and its propagation direction was $31 \pm 6°$S and $94 \pm 4°$E. This implies a radial expansion for this event of 233 km s^{-1}.

Table 4 Positions of STEREO and Earth at 10:07 UT on 21 August 2007.

	STEREO-A	Earth	STEREO-B
Heliocentric radius (AU)	0.9576	1.0117	1.0847
Heliographic (HEEQ) longitude	15.042	0.000	−11.434
Heliographic (HEEQ) latitude	7.340	6.900	6.223
Separation angle with Earth	14.932		11.379
Separation angle A with B		26.311	

The leading-edge plane-of-sky speed calculated from STEREO-A was 623 ± 65 km s^{-1}, whereas the speed from STEREO-B was 713 ± 23 km s^{-1}. Correcting for projection effects returns a true spatial speed of 700 km s^{-1} from STEREO-A and 745 km s^{-1} for STEREO-B, which is in agreement with the speed calculated by geometric localization, given the error estimates. For comparison, CACTus identified a CME in COR2-A and COR2-B, both with a median speed of 735 km s^{-1}. In addition, the LASCO catalog lists a CME observed in C2 and C3 as a partial halo with a linear speed of 1013 km s^{-1}. There were no CMEs listed in SEEDS catalog for this date.

3.4. 21 August 2007

The final CME we consider occurred on 21 August 2007 when the spacecraft separation angle was only 26°. At such a small separation angle, we expect the geometric localization technique to perform poorly, since the quadrilateral area will be approximately three times larger than the actual CME area (Pizzo and Biesecker, 2004). Both spacecraft observed this event as a west-limb event. The CME onset in COR2-A occurred at 07:07 UT, whereas in COR2-B the onset occurred at 10:08 UT. Initial CME identification at STEREO-B is significantly later than at STEREO-A because the COR2-B telescope pointing was offset relative to the other SECCHI-B telescopes, which led to excess brightness at the edge of the COR2-B occulter; this problem has since been corrected. At the time of the CME, the STEREO spacecraft and Earth were at the positions indicated in Table 4 and shown in Figure 11.

Applying the geometric localization technique to observations of this event taken at 13:53 UT yields the three-dimensional spatial location shown in Figure 12. As in Figure 5, the right-hand plot is for an observer hovering over the west limb of the Sun. Notice the extremely large size of the bounding volume because of the small spacecraft separation. Such a large bounding box makes it extremely difficult to identify the shape or orientation of the CME; however, as we shall show, it does not adversely affect the calculation of the centroid or leading-edge velocity. As the STEREO mission continues, and the spacecraft separation becomes greater than 145° after July 2010, the geometric localization technique will again generate large bounding volumes when used only with the STEREO spacecraft. However, if observations from SOHO are also utilized, this problem can be ameliorated.

Figure 13 shows the position as a function of time for the leading edge of the CME. The leading-edge speed was 373 ± 6 km s^{-1} and the propagation direction was 19 ± 1°S and 102 ± 4°W. Note that this places the CME in the plane of sky as seen from STEREO-A. The centroid speed for this CME was 274 ± 13 km s^{-1} and the propagation direction was 11 ± 2°S and 124 ± 4°W. In other words, this event occurred behind the west limb of the Sun as viewed from Earth. The radial expansion for the CME was 99 km s^{-1}.

The leading-edge plane-of-sky speed calculated from STEREO-A was 367 ± 8 km s^{-1}, whereas the speed from STEREO-B was 329 ± 9 km s^{-1}. Correcting for projection effects

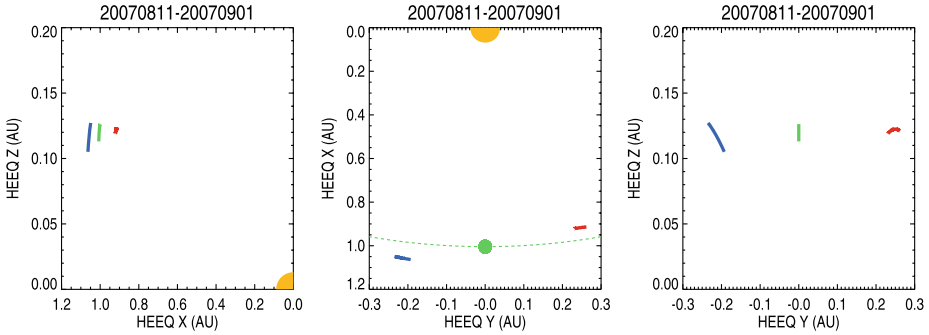

Figure 11 Location of STEREO spacecraft and Earth for a 20-day span centered on 21 August 2007. The use of colors is the same as in Figure 4.

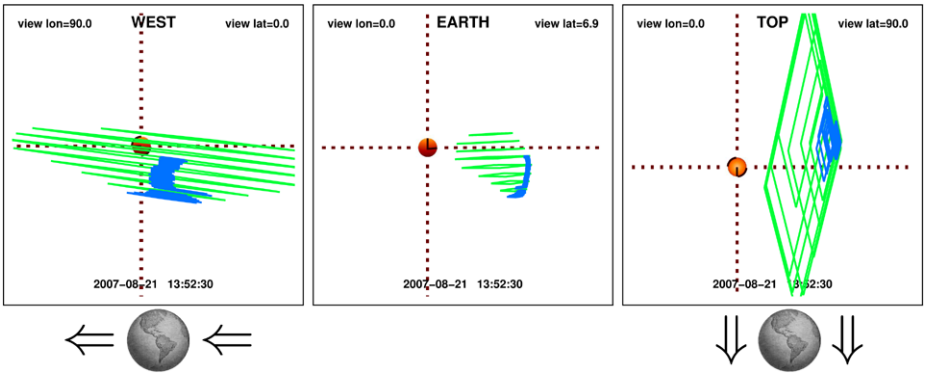

Figure 12 The three-dimensional spatial location of the CME on 21 August 2007 at 13:53 UT as calculated using geometric localization. These plots are similar to those shown in Figure 5.

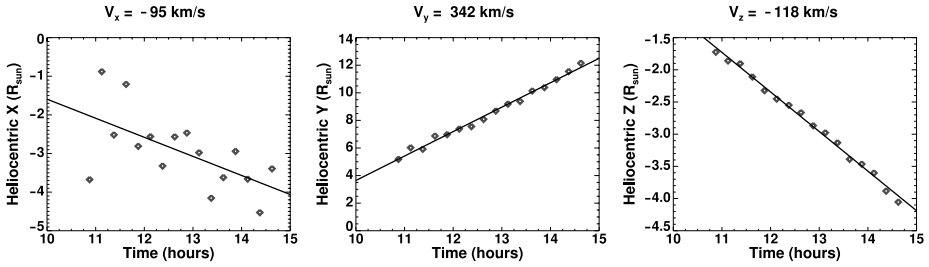

Figure 13 The three-dimensional velocity, in HEEQ coordinates, of the leading edge for the CME observed on 21 August 2007.

returns true spatial speeds of 367 and 358 km s^{-1} from STEREO-A and STEREO-B, respectively. These speeds agree quite well with the speed calculated by geometric localization. For comparison, CACTus identified a CME in COR2-A with a median speed of 357 km s^{-1} and a CME in COR2-B with a median speed of 367 km s^{-1}. LASCO only observed the end of this event, since most of the CME occurred during a data gap. The catalog lists the CME

Table 5 CME speeds in km s^{-1} using various different techniques. The column headers indicate the date of the CME and the position of STEREO-A and STEREO-B and the CME longitude in degrees relative to the Earth – Sun line. The leftmost columns indicate the technique used to obtain the speed, whether the speed is calculated for the CME centroid (cent) or the leading edge (LE), and whether the speed is a radial speed in 3D space or a 2D plane-of-sky (POS) speed. GL denotes geometric localization; ST-[AB] (true) denotes the true-spatial speeds derived from the plane-of-sky speeds for STEREO-[AB]; ST-[AB] denotes the plane-of-sky speeds obtained from STEREO-[AB] as calculated in this paper; CACTus-[AB] denotes the CME speeds obtained from the CACTus catalog using STEREO-[AB] data; SOHO CUA denotes the speed obtained from the LASCO CME catalog at the Catholic University of America; and SOHO SEEDS denotes the CME speed obtained from the SEEDS catalog.

Date	2007-08-21	2007-12-31	2008-01-02	2008-10-17
STEREO-A angle	14.932	21.169	21.202	40.660
STEREO-B angle	−11.379	−22.801	−22.891	−38.465
CME angle	102	−96	−64	−178
GL–cent radial	274 ± 13	491 ± 36	324 ± 45	232 ± 31
GL–LE radial	373 ± 6	724 ± 51	640 ± 64	428 ± 44
ST-A (true)–LE radial	367	700	650	400
ST-B (true)–LE radial	358	745	626	393
ST-A–LE POS	367 ± 8	623 ± 65	648 ± 48	250 ± 23
CACTus-A–POS	357	735	520	231
SOHO CUA–LE POS	567	1013	676	143
SOHO SEEDS–POS	N/A	N/A	350	213
ST-B–LE POS	329 ± 9	713 ± 23	412 ± 53	255 ± 38
CACTus-B–POS	367	735	416	312

speed as 567 km s^{-1} based on three data points in C3. There were no CMEs listed in SEEDS catalog for this date.

4. Conclusions

The geometric localization technique is by its nature inherently robust and straightforward to apply in near-real time. A temporal sequence of highly-compressed STEREO Space Weather Beacon images for a single CME, taken by the COR2 telescope, can be analyzed in less than five minutes. From such an analysis we can readily compute the centroid, leading-edge, and expansion velocities for the CME. Table 5 lists the CME speeds, obtained via geometric localization and from various catalogs, for several events at STEREO spacecraft separation angles ranging from 26° to 79°.

Although at present we have a small sample size, the random error in the computed CME velocity, either for the centroid or leading-edge speed and direction of propagation, does not appear to depend on spacecraft separation. This error, which results from variations in the hand-drawn boundary used to identify the CME in COR2 observations, is frequently less than 10%. Note that the percent error in the radial speed will translate into the same percent error in the transit time of an Earth-directed CME, or equivalently, into the same percent error in the arrival time at Earth of such a CME. For example, by assuming a 10% error in the CME speed, the error in the predicted arrival time at Earth of a 500 km s^{-1} CME would be

approximately 14 hours. For a very fast, and potentially geoeffective, Earth-directed CME, say one with a speed of 2500 km s^{-1}, the predicted arrival time at Earth would have an error of approximately 2 hours, if we assume a 10% error in the speed. However, for such a fast CME the percent error in the speed may be higher because there will be fewer points to use in calculating the CME velocity, and hence one or two outlier points will exert a greater influence on the linear fit.

The geometric localization technique has some limitations; in particular, simulations indicate that the technique does a poor job of characterizing the size and shape of CMEs for spacecraft separations less than 30° or greater than 150°. However, this situation can be improved by using more than two spacecraft views; for example, we can augment the two SECCHI viewpoints with LASCO's perspective. In spite of this minor limitation, the method promises a substantial improvement in our capability to locate and characterize CMEs for forecasting, as well as research purposes. On the research side, accurate statistical knowledge of gross CME properties obtained from geometric localization will enable us to explore associations among solar surface, coronal, and interplanetary structures and disturbances for Earth-directed geoeffective CMEs. On the forecasting side, accurate knowledge of the CME speed and direction of propagation will enable space weather forecasters to determine whether a CME is truly Earth directed, and if so, at what time the CME will impact the geospace environment. In conclusion, we believe that the geometric localization technique is suitable for operational use in the NOAA Space Weather Prediction Center.

Acknowledgements The research at NOAA/SWPC was supported by NASA Living With a Star TR&T grant No. NNH05AB491. This paper uses data from the CACTus CME catalog, generated and maintained by the SIDC at the Royal Observatory of Belgium. This paper also uses data from the SEEDS CME catalog, generated and maintained by the Space Weather Laboratory at George Mason University. The LASCO CME catalog referred to in this paper is generated and maintained at the CDAW Data Center by NASA and The Catholic University of America in cooperation with the Naval Research Laboratory. SOHO is a project of international cooperation between ESA and NASA.

References

Antunes, A., Thernisien, A., Yahil, A.: 2009, Hybrid reconstruction to derive 3D height-time evolution for Coronal Mass Ejections. *Solar Phys.* submitted.

Biesecker, D.A., Webb, D.F., St. Cyr, O.C.: 2008, STEREO space weather and the space weather beacon. *Space Sci. Rev.* **136**, 65. doi:10.1007/s11214-007-9165-7.

Brueckner, G.E., Howard, R.A., Koomen, M.J., Korendyke, C.M., Michels, D.J., Moses, J.D., Socker, D.G., Dere, K.P., Lamy, P.L., Llebaria, A., Bout, M.V., Schwenn, R., Simnett, G.M., Bedford, D.K., Eyles, C.J.: 1995, The Large Angle Spectroscopic Coronagraph (LASCO). *Solar Phys.* **162**, 402.

Domingo, V., Fleck, B., Poland, A.I.: 1995, The SOHO mission: an overview. *Solar Phys.* **162**, 37.

Driesman, A., Hynes, S., Cancro, G.: 2008, The STEREO observatory. *Space Sci. Rev.* **136**, 44. doi:10.1007/s11214-007-9286-z.

Eichstedt, J., Thompson, W.T., St. Cyr, O.C.: 2008, STEREO ground segment, science operations, and data archive. *Space Sci. Rev.* **136**, 626. doi:10.1007/s11214-007-9249-4.

Gosling, J.T.: 1990, Coronal mass ejections and magnetic flux ropes in interplanetary space. In: Russel, C.T., Priest, E.R., Lee, L.C. (eds.) *Physics of Magnetic Flux Ropes, Geophysical Monograph Series* **58**, AGU, Washington, 364.

Howard, R.A., Moses, J.D., Vourlidas, A., Newmark, J.S., Socker, D.G., Plunkett, S.P., Korendyke, C.M., Cook, J.W., Hurley, A., Davila, J.M., Thompson, W.T., St. Cyr, O.C., Mentzell, E., Mehalick, K., Lemen, J.R., Wuelser, J.P., Duncan, D.W., Tarbell, T.D., Wolfson, C.J., Moore, A., Harrison, R.A., Waltham, N.R., Lang, J., Davis, C.J., Eyles, C.J., Mapson-Menard, H., Simnett, G.M., Halain, J.P., Defise, J.M., Mazy, E., Rochus, P., Mercier, R., Ravet, M.F., Delmotte, F., Auchère, F., Delaboudinière, J.P., Bothmer, V., Deutsch, W., Wang, D., Rich, N., Cooper, S., Stephens, V., Maahs, G., Baugh, R., McMullin, D., Carter, T.: 2008, Sun Earth Connection Coronal and Heliospheric Investigation (SECCHI). *Space Sci. Rev.* **136**, 115. doi:10.1007/s11214-008-9341-4.

Kaiser, M.L., Kucera, T.A., Davila, J.M., St. Cyr, O.C., Guhathakurta, M., Christian, E.: 2008, The STEREO mission: an introduction. *Space Sci. Rev.* **136**, 16. doi:10.1007/s11214-007-9277-0.

Moran, T.G., Davila, J.M.: 2004, Three-dimensional polarimetric imaging of coronal mass ejections. *Science* **305**, 70.

Olmedo, O., Zhang, J., Wechsler, H., Poland, A., Borne, K.: 2008, Automatic detection and tracking of coronal mass ejections in coronagraph time series. *Solar Phys.* **248**, 499. doi:10.1007/s11207-007-9104-5.

Pizzo, V.J., Biesecker, D.A.: 2004, Geometric localization of STEREO CMEs. *Geophys. Res. Lett.* **31**. doi:10.1029/2004GL021141.

Robbrecht, E., Berghmans, D.: 2004, Automated recognition of coronal mass ejections (CMES) in near-real-time data. *Astron. Astrophys.* **425**, 1106. doi:10.1051/0004-6361:20041302.

Thernisien, A.F.R., Howard, R.A., Vourlidas, A.: 2006, Modeling of flux rope coronal mass ejections. *Astrophys. J.* **652**, 773.

Thompson, W.T.: 2006, Coordinate systems for solar image data. *Astron. Astrophys.* **449**, 803. doi:10.1051/0004-6361:20054262.

Yashiro, S., Gopalswamy, N., Michalek, G., St.Cyr, O.C., Plunkett, S.P., Rich, N.B., Howard, R.A.: 2004, A catalog of white light coronal mass ejections observed by the SOHO spacecraft. *J. Geophys. Res.* **109** A07105. doi:10.1029/2003JA010282.